調査報告書 23－12

An exploration of air pollution patterns in Japan, South Korea, and China

令和 6（2024）年 2 月

公益財団法人　アジア成長研究所

An exploration of air pollution patterns in Japan, South Korea, and China

Alvaro Domínguez*

*Asian Growth Research Institute, Kitakyushu, Japan.

February 2024

Abstract

We investigate the spatial distribution of air pollutants in Japan, South Korea, and China for the year 2021. Our analysis utilizes satellite data on fine particulate matter at the municipal/county level, along with population density, vegetation difference, and night lights. Using dependence analysis and a clustering method to classify municipalities and counties based on geographical and similar attributes, we delineate distinct clusters within each country. Furthermore, through this spatial examination, we identify consistent positive correlations between air pollution and economic activity in each country. These methods allow us to detect areas where targeted policies can effectively enhance air quality for the population.

Keywords: Air pollution, Japan, South Korea, China, Spatial analysis.

1 Introduction

Historically, as countries undergo economic growth and development, they often experience rapid environmental deterioration. South Korea and China were no exception; during periods of rapid economic growth, their air quality significantly declined. Given their geographical proximity to and economic interdependence with Japan, these nations can draw valuable insights from Japan's experience with environmental deterioration and subsequent improvement after the 1960s. This study adopts a spatial analysis perspective to explore the distribution of air pollution and economic activity

in China, Japan, and South Korea, examining different cities and regions. Through various spatial techniques, we investigate the existence of clusters with similar levels of economic activity and air pollution in these countries.

We employ satellite data from the AidData geoquery database (Goodman et al., 2019) to assess particulate matter ($PM_{2.5}$), health and density of vegetation (NDVI), population density, and night lights. Our focus on $PM_{2.5}$, an easily identifiable air pollutant, eliminates the need to trace its origin, simplifying the study. Using principal component analysis (PCA), spatial dependence analysis, and a spatial clustering algorithm, we identify and analyze clusters of municipalities for Japan and South Korea, and counties for China.[1] All this allows us to detect municipalities/regions within each country with similar economic activity and air pollution levels. Employing PCA, we decrease the dimensionality of the variables into two components: Component one (PC1) includes economic activity-related variables (population density, night lights, and the vegetation index NDVI), while Component two (PC2) primarily consists of $PM_{2.5}$.

Next, we apply the spatial dependence method introduced by Anselin (1995). This enables the identification of regional hot spots (high-value clusters), cold spots (low-value clusters), and spatial outliers. Subsequently, we utilize a spatial clustering method to internally derive regional boundaries based on the pollution levels and economic activity of the municipalities within the studied countries.

In this study, we identify positive and statistically significant levels of spatial dependence for both PC1 and PC2 across various municipalities of Japan and South Korea, and counties in China. The PC1 data highlights clusters with high economic activity. Conversely, the PC2 data reveals clusters with low pollution levels in Honshu's eastern area and high pollution spread throughout the island of Kyushu. In the case of South Korea, a cluster of high pollution levels is located to the northwest, mainly comprising Seoul, and a small cluster of low pollution, primarily to the southwest. In China, a large cluster of low air pollution is located to the northwest, and many smaller clusters of high levels of air pollution are found to the northeast, center, and southwest.

By utilizing the PC1 and PC2 data, we can effectively partition each country into separate analytical regions. These newly defined regions have boundaries that differ from the traditional administrative divisions. As a result, it becomes imperative to devise policies aimed at improving air quality, with a focus on coordinated efforts spanning various municipalities within

[1] Throughout this work, we will use the terms "municipalities" and "counties" interchangeably to economize on words.

these newly established regions in each country.

The impact of air pollution on human health is substantial, ranging from minor upper respiratory irritation to severe outcomes such as lung cancer, chronic bronchitis, and asthmatic attacks (Bernstein et al., 2004; Kampa and Castanas, 2008). An investigation by Lanzi et al. (2018) assesses the potential costs of outdoor air pollution, projecting that if no action is taken, these costs could escalate to reach up to 1% of global GDP by 2060. Additionally, Dechezleprêtre et al. (2019) estimate that an increase of 1 $\mu g/m^3$ in $PM_{2.5}$ concentrations within a given year could result in a 0.8% impact on real GDP.

Several works examine the impact of air quality on the Japanese population. Katanoda et al. (2011) delve into the consequences of sulfur dioxide, nitrogen dioxide, and $PM_{2.5}$ on individuals from three different prefectures, noting significant increases in lung cancer and respiratory diseases due to prolonged exposure to air pollutants. Yorifuji et al. (2015), based on a nationwide population-based longitudinal survey, find that exposure to air pollution during pregnancy increases the likelihood of babies being born with low weight.

Numerous studies employ spatial data to analyze air pollution in Japan. Kume et al. (2007) utilize contour maps to detail the monthly distribution variation of air pollutants for Shizuoka from 2001 to 2002. Araki et al. (2015) utilize regression-kriging to analyze air pollutants from 2009 to 2010, demonstrating that this methodology accurately predicts the spatial distribution of air pollutants in the country with high accuracy and resolution. Furthermore, Shimadera et al. (2009) reveal that transboundary air pollutants originating from neighboring Asian countries significantly impact ionic concentrations in fog in the Kinki region.

For South Korea, Jung et al. (2019) investigate the link between urban structures and air pollutant emissions, considering factors such as size, area, and the configuration of industrial complexes. Utilizing Bayesian spatial linear regression models, the authors reveal varying local emissions in areas with agglomerated industry complexes or large populations. Utilizing province-level data and focusing on the National Strategy for Green Growth Hille et al. (2021) investigates the impact of economic growth on sulfur oxide and total suspended particles (TSP) emissions. The study emphasizes the need for a greener growth path through targeted environmental regulations, cleaner technologies, and a shift towards creative sectors, supported by investments in R&D and education.

Lim et al. (2014) explores cardiovascular mortality's regional distribution, finding higher rates in provincial districts in Incheon and the northern part of Gyeonggido compared to other areas. Kim et al. (2019) highlight that the effects of PM_{10} on mortality may extend beyond a month, with varying

impacts for SO_2. The authors explain that different cities exhibited higher PM_{10} mortality effects, particularly with elevated SO_2 concentrations. Their findings underscore the importance of addressing both particulate (PM_{10}) and gaseous (SO_2) pollution in air quality interventions for effective public health outcomes.

In the context of China, He et al. (2017) conduct a geospatial analysis of inequality spanning various Chinese counties, prefectures, and provinces from 1997 to 2010. Employing local indicators of spatial autocorrelation, they identify a northward shift in hot spots of economic growth. Examining the relationship between the socioeconomic status of Chinese counties and prolonged exposure to $PM_{2.5}$ concentrations, Han et al. (2021) find that populations in economically disadvantaged counties are disproportionately vulnerable to the adverse impacts of such exposure. Yin et al. (2015) investigate the Environmental Kuznets Curve (EKC) hypothesis concerning CO_2 emissions, utilizing panel data from 1999 to 2011 and finding supporting evidence for its existence. Wang et al. (2016) explore the impacts of economic growth and urbanization on sulfur dioxide emissions through the EKC hypothesis, confirming a relationship between economic growth and sulfur dioxide emissions but not for urbanization and the latter.

This paper is structured as follows: The following section explains the data utilized, providing descriptive statistics for the variables under examination. Section 3 unveils the results, while in Section 4, we explore how these methods can be complementary, and discuss relevant policy implications. The paper concludes in Section 5.

2 The Data

2.1 Description of the data

For this work, we rely on a novel dataset on air pollution from the AidData geoquery database (Goodman et al., 2019). More specifically, we use the following variables:

- **Particulate matter ($PM_{2.5}$) concentration:** This metric depicts the presence of gaseous pollutants in micrograms (one-millionth of a gram) per cubic meter ($\mu g/m^3$) of ambient air for the year 2021. These particles can comprise a variety of chemicals, and the primary data originates from Van Donkelaar et al. (2021).

- **Normalized Difference Vegetation Index (NDVI):** This numerical indicator is used in remote sensing and satellite imagery analysis to

assess and quantify vegetation health and density. It helps in assessing changes in vegetation over time, identifying areas affected by drought or deforestation, and providing insights into ecosystem health. Null values represent surfaces like bare soil or rocks, indicating an urban area. The original source of this data is Pedelty et al. (2007).

- **Population density:** This indicator calculates the number of people per square kilometer in 2020. The source of this data is the *CIESIN* (Columbia University, 2018).

- **Night lights:** This indicator communicates the intensity of lights emanating from cities, towns, and other areas with sustained lighting. The measurements are expressed in digital numbers (DNs) for the year 2020, serving as a proxy for the economic activity occurring in a particular area or region. The primary source of this data is Elvidge et al. (2021).

2.2 Descriptive statistics

Tables 1, 2, and 3 provide summary statistics of the previously discussed variables pertaining to Japan, South Korea, and China. We observe that, on average, China has higher $PM_2.5$ concentrations (29.15 $\mu g/m^3$ vs 10.09 $\mu g/m^3$ for Japan and 19.21 $\mu g/m^3$ for South Korea) even though it has a lower population density (535.41 person per km^2 compared to 3732.5 for South Korea and 1103.99 for Japan).

Night lights serve as an indicator due to their strong correlation with economic activity. They are instrumental in examining economic dynamics across different cities and regions. Areas with heightened economic activity, such as urban centers, tend to have brighter lights, while those with lower activity, like rural areas, display dimmer lights.

Figures 1, 2, and 3 provide an overview of the spatial distribution of $PM_{2.5}$ concentrations in Japan, South Korea, and China respectively. Most concentrations in Japan are concentrated in the Kantou region and parts of the Chuubu and Kansai regions. Kyushu, on the other hand, exhibits higher concentration levels in the Fukuoka and Kumamoto areas. For South Korea, the highest concentrations are to the west, in the Gyeonggi province and parts of the South Chungcheong province. In China, a similar pattern is observed in the northeastern and northern regions, as well as in certain areas of the eastern region. For all of the countries analyzed, municipalities with elevated pollution values tend to cluster with others of similar levels and vice versa, although these clusters are not necessarily contiguous.

Table 1: Descriptive statistics for Japan

Statistic	**Mean**	**St. Dev.**	**Min**	**Q1**	**Median**	**Q3**	**Max**	**Obs.**
Particulate matter concentration ($PM_{2.5}$) ($\mu g/m^3$, 2021)	10.09	2.77	0.00	8.64	9.91	11.74	18.69	1665
NDVI, 2020	4354.01	2720.31	2.40	66.19	4561.86	787.48	39792.82	1665
Population density (persons per km^2, 2020)	1103.99	2676.25	2.40	63.72	207.84	784.28	39792.82	1665
Night Lights (DNs, 2020)	3.86	8.10	0.00	0.26	0.88	3.47	77.01	1665

Table 2: Descriptive statistics for South Korea

Statistic	**Mean**	**St. Dev.**	**Min**	**Q1**	**Median**	**Q3**	**Max**	**Obs.**
Particulate matter concentration ($PM_{2.5}$) ($\mu g/m^3$, 2021)	19.21	4.55	0.00	17.78	19.66	21.22	27.96	229
NDVI, 2020	3609.78	1090.26	501.16	2753.82	3803.72	4446.14	5758.87	229
Population density (persons per km^2, 2020)	3732.50	5773.55	16.32	80.51	431.40	5411.36	24765.50	229
Night Lights (DNs, 2020)	15.98	19.79	0.33	1.56	5.09	28.69	101.08	229

Table 3: Descriptive statistics for China

Statistic	**Mean**	**St. Dev.**	**Min**	**Q1**	**Median**	**Q3**	**Max**	**Obs.**
Particulate matter concentration ($PM_{2.5}$) ($\mu g/m^3$, 2021)	29.15	11.35	0.00	22.09	27.70	35.81	88.44	2391
NDVI, 2020	4278.76	1196.51	153.71	3630.69	4339.67	5171.08	7092.75	2391
Population density (persons per km^2, 2020)	535.41	1092.85	0.05	95.33	232.35	537.60	15907.00	2391
Night Lights (DNs, 2020)	1.73	4.07	0.00	0.11	0.39	1.27	63.17	2391

Figure 1: $PM_{2.5}$ concentrations in Japan

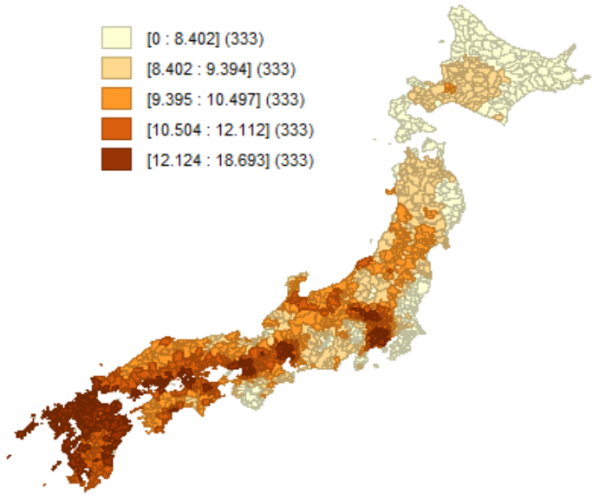

Figure 2: $PM_{2.5}$ concentrations in South Korea

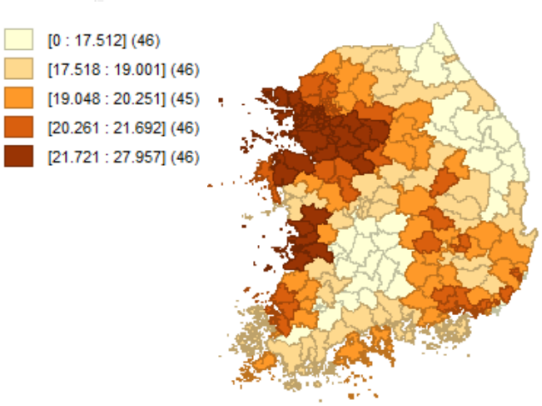

Figure 3: $PM_{2.5}$ concentrations in China

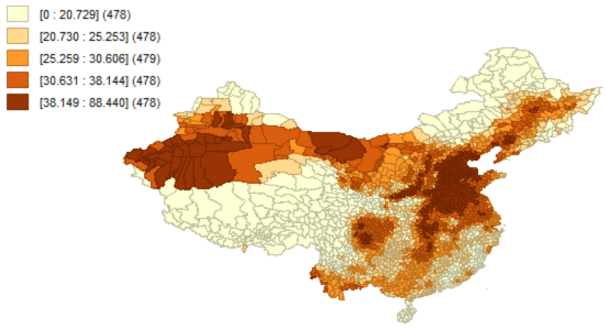

3 Results

3.1 Principal Component Analysis

Table 4 presents a condensed overview of the outcomes from the principal component analysis. The table information delineates the findings for each country and is structured into three sections. First, we show the proportion of variance, as obtained from the principal components. We denote the first component as PC1 and the second one as PC2. These components illustrate the variance for Japan, Korea, and China. With regard to Japan, PC1 and PC2 account for 59% and 23% of the total variance. For South Korea, PC1 represents 61%, while PC2 contributes 25%. Lastly, in the case of China, PC1 explains 50% of total variance and PC2 27%. Cumulatively, these components represent upwards of 75% of the total variance.

The second section details the squared correlations between the components and the original variables. This information provides insights into the magnitude of correlations, enabling an examination of the components concerning the original variables. For instance, key variables constituting PC1 for all the countries include NDVI and night lights. In PC2, the most significant variable is particulate matter. To determine the number of components to utilize, we adhere to the "95% threshold criterion." This numerical value corresponds to the components necessary to explain 95% of the variance. In our context, this implies utilizing the first two components.

Having condensed the variables into PC1 and PC2 to capture a substantial portion of the variance and reduce dimensionality, we can proceed to examine their spatial distribution. We then delve into the analysis of their spatial dependence.

Table 4: Principal Component Analysis

Total Variance and Cumulative Proportion												
	Japan				**South Korea**				**China**			
	PC1	**PC2**	**PC3**	**PC4**	**PC1**	**PC2**	**PC3**	**PC4**	**PC1**	**PC2**	**PC3**	**PC4**
Proportion of variance	0.59	0.23	0.14	0.04	0.61	0.25	0.12	0.03	0.50	0.27	0.20	0.03
Cumulative proportion	0.59	0.82	0.96	1.00	0.61	0.85	0.97	1.00	0.50	0.77	0.97	1.00
Squared correlations between the components and the variables:												
Particulate matter ($PM_{2.5}$)	0.16	**0.81**	0.04	0.00	0.02	**0.98**	0.00	0.00	0.13	**0.44**	0.43	0.00
Population density	**0.83**	0.01	0.10	0.07	**0.66**	0.00	0.33	0.00	0.11	**0.50**	0.39	0.00
NDVI	**0.50**	0.11	0.38	0.00	**0.85**	0.00	0.10	0.05	**0.88**	0.07	0.00	0.06
Night lights	**0.86**	0.00	0.06	0.07	**0.90**	0.01	0.03	0.06	**0.88**	0.06	0.00	0.06
Criterion to choose the number of components												
Eigenvalues:	2.35	0.93	0.58	0.14	2.42	0.99	0.47	0.11	2.00	1.07	0.82	0.11
95% threshold criterion:	2				2				2			

3.2 Spatial Dependence Analysis

Figures 4, 6, and 8, examine the Local Moran scatter plots illustrating autocorrelation for Japan, South Korea, and China, respectively. The X-axis in these plots represents the values of PC1 on the left side and PC2 on the right side, respectively. Meanwhile, the Y-axis displays the weighted mean of the neighbors, indicating the spatial lag. The regression line in these graphs indicates the level of spatial dependence. The Moran scatter plot is divided into four quadrants: top-right, top-left, bottom-right, and bottom-left. The top-right and bottom-left quadrants highlight spatial clusters, emphasizing municipalities and their neighbors with similar high or low values in PC1 and PC2, respectively. Spatial outliers are observed in the top-left and bottom-right parts of the graphs. These outliers represent municipalities with high values in PC1 and PC2, surrounded by neighbors with low values, or vice versa.

The highlighted dots in these Figures indicate observations that are statistically significant (with a p-value of 0.01). This approach mitigates any potential issues related to the multiple comparisons problem. As per Anselin (1995), the multiple comparisons problem is a concern that may arise when conducting any analysis of local indicators of spatial association (LISA).

Figures 5, 7, and 9 display the spatial distribution of municipalities that hold statistical significance for each of the countries we study. The four quadrants in the Moran scatter plots show that the municipalities are grouped into clusters representing hot spots (high-high) and cold spots (low-low) for PC1 and PC2, respectively. The remaining municipalities are characterized as spatial outliers. Figures 4-9 reveal the presence of positive and statistically significant spatial dependence. The Global Moran's I quantifies this spatial relationship. We observe that for all countries, the Global Moran's I for PC2 (representing levels of $PM_{2.5}$) tends to be above 0.5, meaning there is a high

spatial dependence.

In Japan, the coefficient value for PC2 is 0.626; for South Korea, it is 0.530; and for China, 0.835. These coefficients indicate a pronounced spatial dependence. Figure 5b for Japan illustrates clusters of hot spots in the islands of Kyushu and southwest Honshu, comprising 161 municipalities. Figure 7b, shows hot spots in 24 districts in South Korea, mainly from the Gyeonggi Province. Meanwhile, Figure 9b presents hot spot clusters, concentrated mostly in the northwest, center, and southwest regions. All these hot spots exhibit municipalities or districts with elevated mean levels of $PM_{2.5}$ concentrations, surrounded by other municipalities/districts with high levels of $PM_{2.5}$ concentrations.

Conversely, cold spots in Japan consist of 66 municipalities, mostly gathered to the east in the Kanto region. Others surround these municipalities with lower levels of $PM_{2.5}$ concentration. In the same vein, in South Korea, we observe that a tiny cold spot of 6 districts is located in the southeast part of the country (in the city of Busan). For China, a large cold spot is located to the northwest, with a medium-sized one to the east.

Figures 5a, 7a, and 9a illustrate the spatial dependence of PC1 in Japan, South Korea, and China respectively. We observe a positive and statistically significant spatial dependence, which is higher than its PC2 counterpart, except for China. The corresponding values for this dependency are 0.881, 0.828, and 0.404, respectively. In Japan, PC2's hot spots are limited, primarily located in parts of the Tokyo, Kansai, and Chugoku regions, encompassing 112 municipalities. In contrast, cold spots are more extensive, spanning most of the island of Hokkaido, large parts of the northeast and south west of the Honshu island. Similar to Japan, South Korea exhibits reduced hotspots for PC1, focused chiefly in the cities of Seoul to the northwest, and Busan to the southeast. On the other hand, South Korea's coldspots for its PC1 variable is large and extends most of the north and also parts of the south. Finally, for China, we see small pockets of hotspots in the middle, east and south regions. As in the cases of Japan and South Korea, coldspots are rather large, spreading through the northeast, southeast, and center regions.

The Moran scatter plot functions as a tool for identifying two-dimensional clusters. The first dimension represents the values of principal components, such as economic activity and air pollution, while the second dimension reflects spatial contiguity, i.e., the geographical proximity of municipalities. Ideally, we would like to classify the areas shaded in grey on the maps (Figures 5, 7, and 9) that lack statistical significance. To address this, we employ a spectral clustering method in the following section.

3.3 Spectral Clustering

Next, we employ spectral clustering, a technique for partitioning graphs that works well with both dimension reduction and cluster identification simultaneously. Spectral clustering can be conceptualized as the task of dividing a graph into internally cohesive subgraphs while minimizing connections between them. It seeks to optimize the similarity within each cluster. Ideally, these subgraphs should be connected components, entirely internally connected without any links to other subgraphs, but this is rarely achievable in practice. Therefore, the focus shifts to identifying optimal cuts in the graph that result in a partition of k subsets, prioritizing high internal connectivity and low inter-cluster connectivity.

Through the Spectral clustering method, it becomes feasible to partition various regions into analytical groupings based on their level of economic activity and/or air pollution. In contrast to conventional regional divisions, which merely provide information on locational similarity, partitioning the countries into analytical regions yields additional insights into both their locational and attribute similarities. It may be the case that municipalities exhibit locational similarity while differing in attributes such as pollution levels or economic activity. Figures 10-12 depict analytical regions comprising clusters of municipalities characterized by similar pollution levels and/or economic activity, along with spatial heterogeneity within each administrative region.

Two key observations emerge from the clustering process. First, both economic activity and air pollution levels (represented by PC1 and PC2, respectively) extend across multiple administrative regions. This underscores the need for coordination among the affected regions in each country to address and ameliorate the situation. Second, it is noteworthy that certain countries exhibit more significant spatial variation and heterogeneity than others. This is due to the intrinsic spatial distribution of the variables under analysis in each country.

Japan has improved its air quality significantly in recent decades. The results show that very few municipalities do not attain the environmental quality standards that the Ministry of the Environment set. These annual quality standards call for concentrations of $PM_{2.5}$ to be less than or equal to 15.0 $\mu g/m^3$.[2] Currently, only some municipalities located on the island of Kyushu cross this threshold (shown in Figure 10b), but with a downward trend. This implies that should this tendency persist, they will also comply with the environmental quality standards in a few years.

[2]https://www.env.go.jp/en/air/aq/aq.html

In the case of China, we see in Figure 3 that to the east and the center-west $PM_{2.5}$ concentrations are quite high. Yousefi et al. (2023) explain that $PM_{2.5}$ levels saw a notable increase across all regions from 1980 to 2020. Notably, the eastern and southern regions experienced the most significant upward trends in $PM_{2.5}$ concentrations. However, around 2007, the $PM_{2.5}$ concentration trends shifted from upward to downward in these regions due to the implementation of air pollution control policies by the Chinese government. The clustering analysis (shown in Figure 12b) highlights this through the partitioning of the country into analytical regions, with the east in red and south in blue being the regions where more commitment needs to be made.

Despite the efforts made in recent decades to reduce domestic air pollution, South Korea still grapples with frequent and severe air pollution during the winter and spring months, posing significant risks to public health and socioeconomic activities. It is recognized that the air quality in South Korea is impacted not only by local stationary and mobile sources but also by the long-range transport of air pollutants from external origins, such as the airborne particles originating from the industrial activities of China's factories and coal-fired power plants, often referred to as yellow dust (Jun and Gu, 2023).

By gaining a more comprehensive understanding of the spatial interaction of multiple variables, we can enhance our ability to effectively convey strategies for addressing these issues to policymakers and stakeholders. A nuanced comprehension of how pollution is distributed across different regions enables policymakers to devise and tailor policies with greater precision, thereby enhancing their effectiveness in addressing environmental concerns.

4 Discussion and policy implications

The preceding subsections demonstrate that both the Local Moran and Spectral clustering methods serve as complementary analyses. While the Local Moran analysis identifies hot spots and cold spots, the spectral clustering method groups the remaining municipalities into clusters with similar attributes. Utilizing these techniques does not always result in a direct overlay of clusters. Nevertheless, such an analysis aids in identifying robust spatial clusters deserving of further investigation. These clusters offer valuable insights at both the local/regional and national levels for policymakers, assisting in the planning and formulation of policies targeted towards areas where improving air pollution may be desirable.

When comparing the resulting spatial clusters, two considerations must

be kept in mind. First, the Local Moran method assesses observations solely from the high-high and low-low quadrants of the graph, whereas the Spectral clustering incorporates all quadrants. Second, clusters derived from the Spectral method tend to exhibit larger sizes compared to those from the Local Moran method. This disparity arises because the Local Moran method examines spatial contiguity primarily through first-order neighbors, whereas the Spectral clustering method considers higher-order neighbors as well. Consequently, these methodologies complement each other effectively. By leveraging both approaches, we gain insights from the distinct information they offer.

Utilizing a spatial clustering approach allows us to track the differences in $PM_{2.5}$ throughout regions in each of the countries under study. Moreover, pollutants such as $PM_{2.5}$ can travel considerable distances via wind, impacting both distant regions and other countries. Thus, it is imperative for policymakers to foster both inter-regional and international cooperation to effectively address these challenges. As shown in this study, spatial clustering analysis proves instrumental in identifying clusters of regions where collaboration can yield positive outcomes. Conducting such analysis offers a holistic perspective on how regions should be considered, aiding policymakers in making informed decisions.

According to Jun and Gu (2023), approximately 40% of domestic $PM_{2.5}$ concentrations in South Korea, on average, stem from long-range transport from Chinese cities during periods of high $PM_{2.5}$ levels. This underscores the importance of controlling emission releases at their source in China to mitigate air pollution in Korea. Furthermore, the significant impact of long-range transport on the Seoul Metropolitan Area (SMA), where over half of the nation's population resides, suggests that residents in this area may endure the most severe health consequences from exposure to long-range transport. Therefore, it is fundamental to have active diplomatic efforts between Korea and China, alongside the development of corresponding emission reduction policies.

Research by Kaneyasu et al. (2020) shows that many sources of $PM_{2.5}$ in Japan stem from coal and oil combustion by industries, transportation, and heating systems. Furthermore, as noted by Yim et al. (2019), there is evidence of transboundary air pollution from neighboring countries. In this latter case, it is imperative to tackle the air pollution sources for the situation to improve. This presents opportunities for collaborative efforts to improve the environmental quality while fostering economic ties for all the parties involved.

Several policies and regulations could potentially alter these pollution patterns. Firstly, enhancing and expanding the monitoring system for data

collection to study and implement measures for $PM_{2.5}$ pollution. Secondly, implementing taxes and subsidies to promote larger shares of cars sold that meet more stringent environmental standards by 2030. Last and fundamentally, international cooperation between Japan, South Korea, and China through joint research and efforts in cutting $PM_{2.5}$ concentrations can have a substantial impact on decreasing air pollution levels. The experience that Japan has accumulated since the 1960s in reducing its air pollution can be of use to China and South Korea. Improving air quality in the latter two countries would also yield benefits to Japan, as it would experience reduced inbound air pollution from these nations.

5 Conclusions

In this study, we identify clusters of municipalities in Japan and South Korea and counties in China. These exhibit similar pollution levels and economic activity to their neighbors. We employ principal component analysis (PCA) and spatial data analysis techniques to achieve this. We then assess regional disparities in $PM_{2.5}$ concentration, population density, night lights, and vegetation concentration. Through PCA, we reduce the dimensionality of these variables into PC1 and PC2. PC1 primarily reflects municipal variations in vegetation, population density, and night lights. Meanwhile, PC2 represents variations in air pollution, specifically $PM_{2.5}$. Subsequently, we identify clusters of municipalities sharing similar economic activity and air pollution levels.

We observe a clear and statistically significant spatial dependence across regions in each country. Municipalities/counties tend to exhibit similar economic activity and air pollution, as indicated by PC1 and PC2, respectively, particularly with other neighboring municipalities/counties. For example, the PC1 hot spot clusters in metropolitan areas like Tokyo, Nagoya, and Osaka in Japan and Seoul and Busan in South Korea are particularly interesting. High levels of economic activity and population density characterize these clusters.

Relying on a Spectral clustering method, we obtain outcomes that largely correspond to those from the spatial dependence analysis. This algorithm partitions each country into different regions based on the results derived from the PC1 and PC2 variables. These newly delineated regions help in indicating the spread of pollution and economic activities across municipal and regional borders. By defining these new boundaries, municipalities in each country can collaborate more effectively in devising and implementing policies to address air pollution issues.

Future research could focus on understanding the clustering of regions throughout multiple periods of time. Additionally, exploring alternative clustering methods that account for changes in regional composition, such as variations in population density and economic activity, may offer deeper insights into the complex relationship between pollution and regional economic development.

6 Appendix

6.1 Figures

Figure 4: Spatial Autocorrelation for Japan

(a) PC1

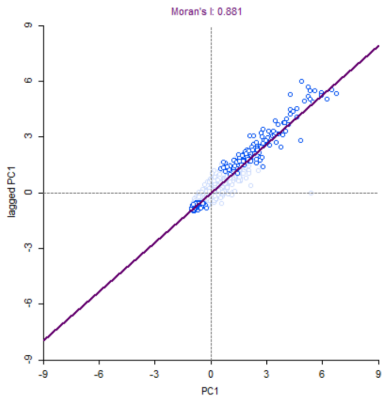

(b) PC2

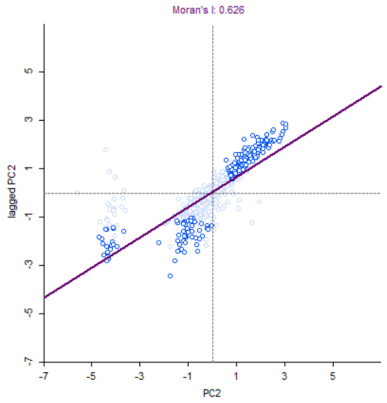

Figure 5: Japanese Hot and Cold Spots (PC1 & PC2)

(a) PC1

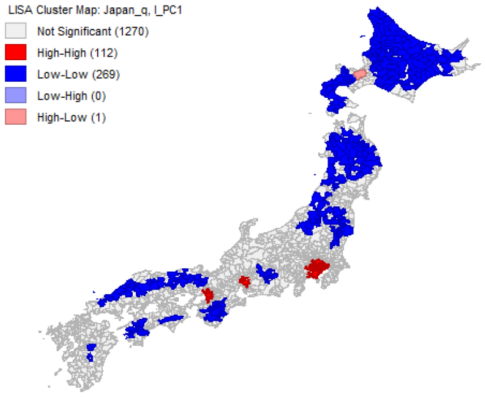

(b) PC2

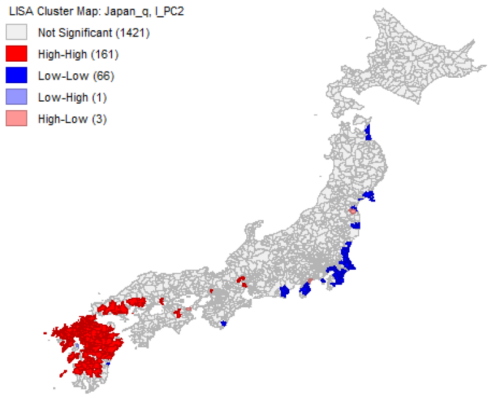

Figure 6: Spatial Autocorrelation for South Korea

(a) PC1

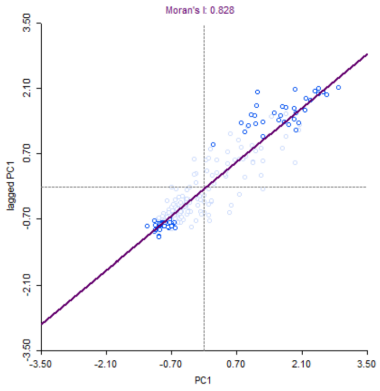

(b) PC2

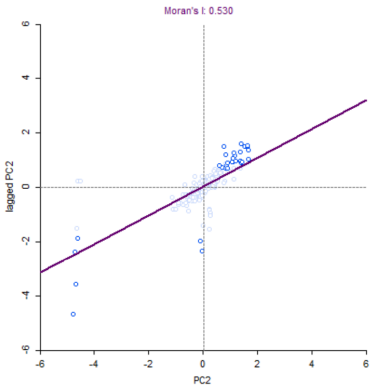

Figure 7: South Korean Hot and Cold Spots (PC1 & PC2)

(a) PC1

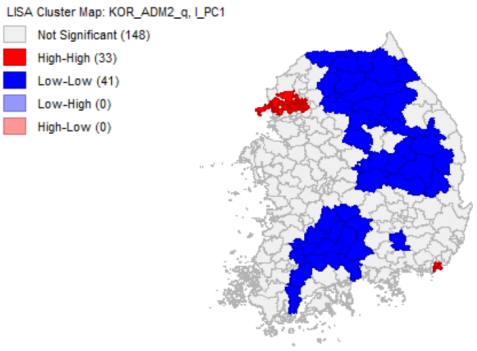

(b) PC2

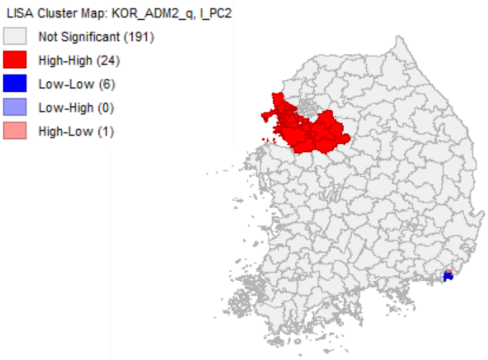

Figure 8: Spatial Autocorrelation for China

(a) PC1

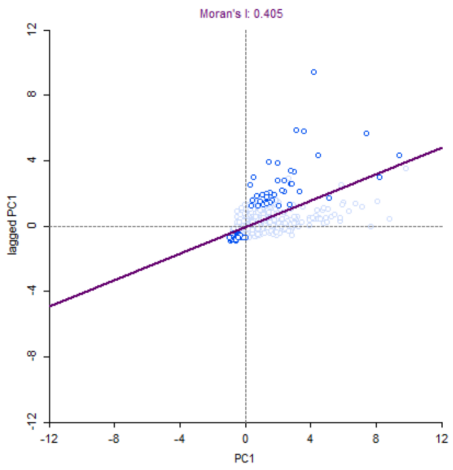

(b) PC2

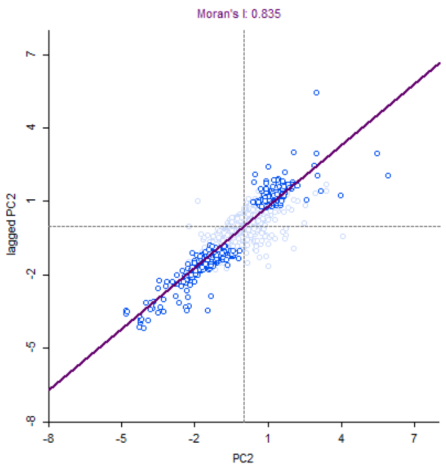

Figure 9: Chinese Hot and Cold Spots (PC1 & PC2)

(a) PC1

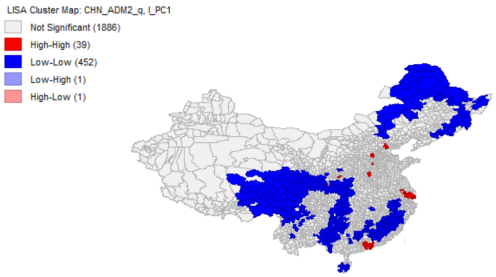

(b) PC2

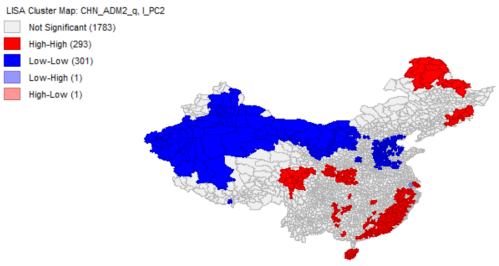

Figure 10: Analytical Regions for Japan

(a) PC1

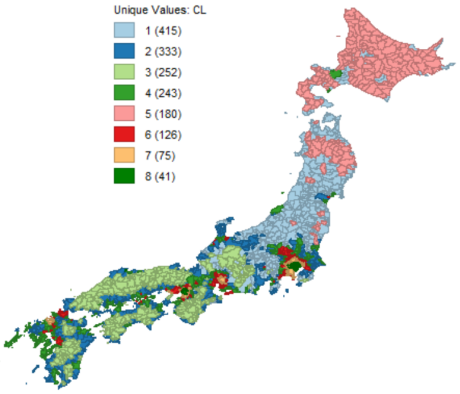

(b) PC2

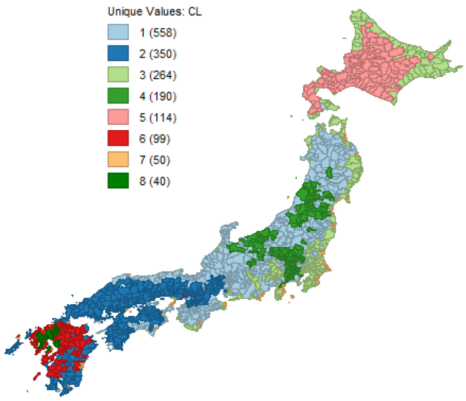

Figure 11: Analytical Regions for South Korea

(a) PC1

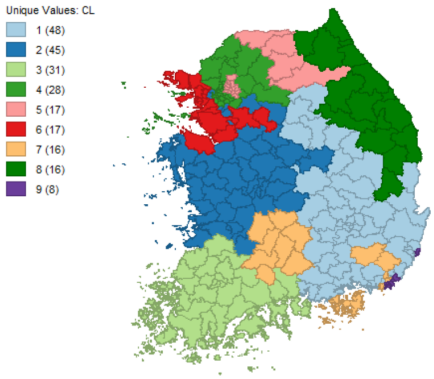

(b) PC2

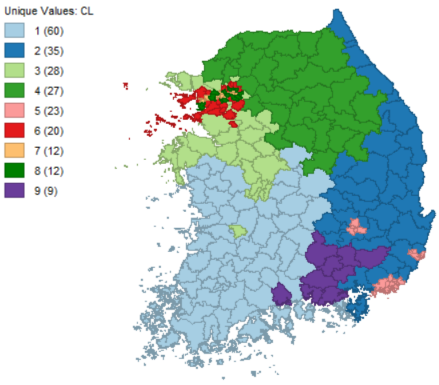

Figure 12: Analytical Regions for China

(a) PC1

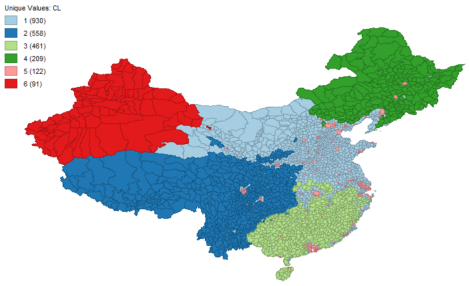

(b) PC2

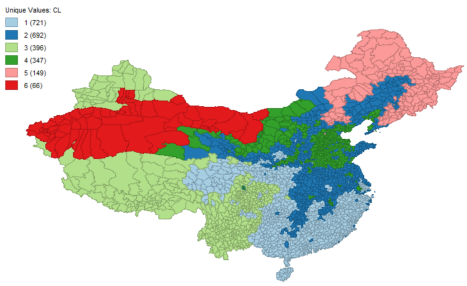

References

Anselin, L. (1995). Local indicators of spatial association—lisa. *Geographical analysis*, 27(2):93–115.

Araki, S., Yamamoto, K., Kondo, A., et al. (2015). Application of regression kriging to air pollutant concentrations in japan with high spatial resolution. *Aerosol and Air Quality Research*, 15(1):234–241.

Bernstein, J. A., Alexis, N., Barnes, C., Bernstein, I. L., Nel, A., Peden, D., Diaz-Sanchez, D., Tarlo, S. M., and Williams, P. B. (2004). Health effects of air pollution. *Journal of allergy and clinical immunology*, 114(5):1116–1123.

Columbia University, C. f. I. E. S. I. N. . C. (2018). Gridded population of the world, version 4 (gpwv4): Population density adjusted to match 2015 revision un wpp country totals, revision 11.

Dechezleprêtre, A., Rivers, N., and Stadler, B. (2019). The economic cost of air pollution: Evidence from europe. *OECD Economics Department Working Papers*.

Elvidge, C. D., Zhizhin, M., Ghosh, T., Hsu, F.-C., and Taneja, J. (2021). Annual time series of global viirs nighttime lights derived from monthly averages: 2012 to 2019. *Remote Sensing*, 13(5):922.

Goodman, S., BenYishay, A., Lv, Z., and Runfola, D. (2019). Geoquery: Integrating hpc systems and public web-based geospatial data tools. *Computers & geosciences*, 122:103–112.

Han, C., Xu, R., Gao, C. X., Yu, W., Zhang, Y., Han, K., Yu, P., Guo, Y., and Li, S. (2021). Socioeconomic disparity in the association between long-term exposure to pm2. 5 and mortality in 2640 chinese counties. *Environment international*, 146:106241.

He, S., Fang, C., and Zhang, W. (2017). A geospatial analysis of multi-scalar regional inequality in china and in metropolitan regions. *Applied Geography*, 88:199–212.

Hille, E., Lambernd, B., and Tiwari, A. K. (2021). Any signs of green growth? a spatial panel analysis of regional air pollution in south korea. *Environmental and Resource Economics*, 80:719–760.

Jun, M.-J. and Gu, Y. (2023). Effects of transboundary pm2. 5 transported from china on the regional pm2. 5 concentrations in south korea: A spatial panel-data analysis. *Plos one*, 18(4):e0281988.

Jung, M. C., Park, J., and Kim, S. (2019). Spatial relationships between urban structures and air pollution in korea. *Sustainability*, 11(2):476.

Kampa, M. and Castanas, E. (2008). Human health effects of air pollution. *Environmental pollution*, 151(2):362–367.

Kaneyasu, N., Ishidoya, S., Terao, Y., Mizuno, Y., and Sugawara, H. (2020). Estimation of pm2. 5 emission sources in the tokyo metropolitan area by simultaneous measurements of particle elements and oxidative ratio in air. *ACS Earth and Space Chemistry*, 4(2):297–304.

Katanoda, K., Sobue, T., Satoh, H., Tajima, K., Suzuki, T., Nakatsuka, H., Takezaki, T., Nakayama, T., Nitta, H., Tanabe, K., et al. (2011). An association between long-term exposure to ambient air pollution and mortality from lung cancer and respiratory diseases in japan. *Journal of epidemiology*, pages 1102090211–1102090211.

Kim, H., Kim, H., and Lee, J.-T. (2019). Spatial variation in lag structure in the short-term effects of air pollution on mortality in seven major south korean cities, 2006–2013. *Environment International*, 125:595–605.

Kume, K., Ohura, T., Noda, T., Amagai, T., and Fusaya, M. (2007). Seasonal and spatial trends of suspended-particle associated polycyclic aromatic hydrocarbons in urban shizuoka, japan. *Journal of hazardous materials*, 144(1-2):513–521.

Lanzi, E., Dellink, R., and Chateau, J. (2018). The sectoral and regional economic consequences of outdoor air pollution to 2060. *Energy Economics*, 71:89–113.

Lim, Y.-R., Bae, H.-J., Lim, Y.-H., Yu, S., Kim, G.-B., and Cho, Y.-S. (2014). Spatial analysis of pm10 and cardiovascular mortality in the seoul metropolitan area. *Environmental health and toxicology*, 29.

Pedelty, J., Devadiga, S., Masuoka, E., Brown, M., Pinzon, J., Tucker, C., Vermote, E., Prince, S., Nagol, J., Justice, C., et al. (2007). Generating a long-term land data record from the avhrr and modis instruments. In *2007 IEEE international Geoscience and remote sensing Symposium*, pages 1021–1025. IEEE.

Shimadera, H., Kondo, A., Kaga, A., Shrestha, K. L., and Inoue, Y. (2009). Contribution of transboundary air pollution to ionic concentrations in fog in the kinki region of japan. *Atmospheric Environment*, 43(37):5894–5907.

Van Donkelaar, A., Hammer, M. S., Bindle, L., Brauer, M., Brook, J. R., Garay, M. J., Hsu, N. C., Kalashnikova, O. V., Kahn, R. A., Lee, C., et al. (2021). Monthly global estimates of fine particulate matter and their uncertainty. *Environmental Science & Technology*, 55(22):15287–15300.

Wang, Y., Han, R., and Kubota, J. (2016). Is there an environmental kuznets curve for so_2 emissions? a semi-parametric panel data analysis for china. *Renewable and Sustainable Energy Reviews*, 54:1182–1188.

Yim, S. H. L., Gu, Y., Shapiro, M. A., and Stephens, B. (2019). Air quality and acid deposition impacts of local emissions and transboundary air pollution in japan and south korea. *Atmospheric Chemistry and Physics*, 19(20):13309–13323.

Yin, J., Zheng, M., and Chen, J. (2015). The effects of environmental regulation and technical progress on co2 kuznets curve: An evidence from china. *Energy Policy*, 77:97–108.

Yorifuji, T., Kashima, S., and Doi, H. (2015). Outdoor air pollution and term low birth weight in japan. *Environment international*, 74:106–111.

Yousefi, R., Shaheen, A., Wang, F., Ge, Q., Wu, R., Lelieveld, J., Wang, J., and Su, X. (2023). Fine particulate matter (pm2. 5) trends from land surface changes and air pollution policies in china during 1980–2020. *Journal of environmental management*, 326:116847.

An exploration of air pollution patterns in Japan, South Korea, and China

令和 6 年 2 月発行

発行所　公益財団法人アジア成長研究所
〒803-0814　北九州市小倉北区大手町 11 番 4 号
Tel：093-583-6202／Fax：093-583-6576
URL：https://www.agi.or.jp
E-mail：office@agi.or.jp